

UC Santa Barbara

UC Santa Barbara Previously Published Works

Title

Rate-Dependent Stiffness and Recovery in Interpenetrating Network Hydrogels through Sacrificial Metal Coordination Bonds

Permalink

<https://escholarship.org/uc/item/19g7j5p8>

Journal

ACS Macro Letters, 4(11)

ISSN

2161-1653

Authors

Menyo, Matthew S
Hawker, Craig J
Waite, J Herbert

Publication Date

2015-11-17

DOI

10.1021/acsmacrolett.5b00664

Peer reviewed

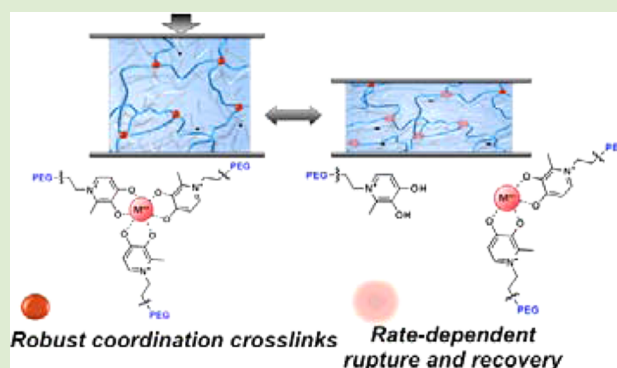
Rate-Dependent Stiffness and Recovery in Interpenetrating Network Hydrogels through Sacrificial Metal Coordination Bonds

Matthew S. Menyo,[†] Craig J. Hawker,[‡] and J. Herbert Waite^{*,†,§}

[†]Graduate Program in Biomolecular Science and Engineering, [‡]Materials Research Laboratory, and [§]Marine Science Institute, University of California, Santa Barbara, California 93106, United States

Supporting Information

ABSTRACT: Four-arm poly(ethylene glycol) (PEG) star polymers modified with 3-hydroxy-4-pyridinone (HOPO) end groups were shown to form transient, coordination networks upon addition of trivalent cations In^{3+} , Fe^{3+} , and Al^{3+} . These coordination-based hydrogels exhibited high activation energies of viscoelasticity (34 kT) and characteristic bond lifetimes tunable over 2 orders of magnitude and could be incorporated into poly(hydroxyethylacrylamide)-based covalent scaffolds to create interpenetrating network hydrogels. Measurements carried out in compression and tension demonstrate that the secondary coordination network imparts toughness and stiffness to the overall material, and unlike traditional interpenetrating networks (IPNs), the extent of toughening is dependent on the rate at which the materials are deformed. The dynamic character of the coordination network also allows recovery after mechanical damage following high amplitude strains.



Natural systems that are deployed in environments exposed to cyclic strain events often show yield behavior and recoverable hysteresis attributed to the sacrificial rupture of metal coordination bonds.¹ For example, Dopa- and His-metal coordination bonds have been shown to provide vital mechanical contributions to the attachment threads of mussels (genus *Mytilus*).^{2–6} Recently, Ashton and Stewart have also shown that Ca^{2+} -phosphate and -carboxylate complexes contribute key roles in the yield and recovery for threads from the larval form of the caddisfly *Hesperophylax occidentalis*.⁷

Metal coordination bonds impart unique, desirable structural properties such as dynamic exchangeability and an inherent capacity for self-healing and recovery. The time scale of this lability is tied to the dissociation kinetics of the complex, which can be varied by metal ion, ligand, pH, and solvent.^{8–12} Craig et al. investigated the mechanical properties of 4-vinylpyridine in DMSO, showing that the incorporation of transient Pd(II)- and Pt(II)-pincer cross-links result in the formation of organogels with viscoelastic properties dependent on ligand dissociation kinetics.^{13,14}

The strength of metal coordination complexes as measured by $\Delta G_{\text{complex}}$ varies widely, from negligible in very weakly chelating systems to >100 kT for strongly chelating metal-ligand pairs like catechol- Fe^{3+} .¹⁵ As with other noncovalent strategies, substantial mechanical reinforcement generally requires the additive or cooperative domain effects from high amounts of lower-affinity complexes such as M^{n+} -carboxylate,^{16,17} Cu^{2+} -nitrilotriacetic acid,¹⁸ or Ca^{2+} -alginate systems.¹⁹ Recently, several studies have shown that robust hydrogels can be formed by functionalizing with small amounts

of high-affinity, biologically inspired Dopa- M^{3+} or His- M^{2+} complexes.^{10–12,20}

We have demonstrated previously the utility of 3-hydroxy-4-pyridinone (HOPO) chelating moieties as dynamic cross-linkers in hydrogels under physiological conditions.²¹ Hydrogels constructed from four-arm poly(ethylene glycol) (tetra-PEG) molecules end-functionalized with HOPO moieties and hard metal ions showed efficient cross-linking, pH-responsive viscoelasticity, and stable dynamic behavior. However, the short, extended hydrogel chain architecture and the wholly dynamic nature of this system resulted in brittle hydrogels with no elastic recovery force.

Interpenetrating double network hydrogel constructs have been shown to lead to dramatic increases in toughness.^{22,23} In this work, we show that the incorporation of a coordination network into a loosely cross-linked hydroxyethylacrylamide covalent scaffold allows the formation of an interpenetrating network (IPN) hydrogel in which the coordination network serves as a sacrificial, energy-dispersive component (Figure 1). The choice of the stable, high-affinity HOPO functionality as a chelating group imparts substantive mechanical reinforcement at low incorporations and in the presence of competing buffer salts. By employing three metal ions with different dissociation rates, we demonstrate reinforced hydrogels with strain-rate-dependent mechanical properties and tunable recovery kinetics.

Received: September 11, 2015

Accepted: October 13, 2015

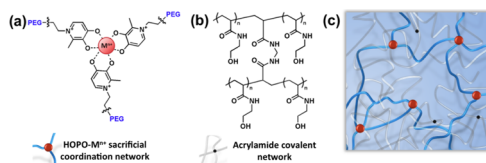


Figure 1. Chemical structures for the (a) 3-hydroxy-4-pyridinone (HOPO)- M^{n+} -based PEG coordination network and (b) poly-(hydroxyethylacrylamide-methylene bis(acrylamide))-based covalently cross-linked networks and (c) interpenetrating network.

Covalent networks were synthesized by polymerization of a hydroxyethylacrylamide solution containing 0.0005 equiv of methylene bis(acrylamide) cross-linker in sealed syringe bodies or Teflon molds (Figure 1). The polymeric cross-linker which forms the basis of the coordination network was prepared by reaction of the amino-functionalized 2-methyl 3-hydroxy-4-pyridinone (HOPO) ligand with an activated four-arm poly(ethylene glycol) (M_w : 10 000 g/mol). This reaction led to a high degree of chain-end functionalization (95% by ^1H NMR integration, Figure S1). Coordination-based hydrogels (10 wt % polymer) were then formed in a three-step process. The HOPO-functionalized PEG star is dissolved in deionized water followed by addition of a small volume of trivalent metal chloride stock solution to achieve a 3:1 HOPO: M^{n+} ratio. Key to the success of this approach is that at $\text{pH} < 4$ the metals are bound in low stoichiometry mono and bis complexes leading to soluble materials. Gelation is triggered upon addition of 1 M NaOH to achieve the desired pH 8.2.

Interpenetrating network hydrogels were formed via an analogous process. The hydroxyethylacrylamide gel was miscible with functionalized tetraPEG at up to 20 wt %, but the radical scavenging nature of the HOPO moieties inhibited polymerization of the network in the presence of the functionalized tetraPEG. To ensure a consistent degree of polymerization, functionalized tetraPEG with monocoordinated metal was introduced by diffusion into the preformed, dehydrated covalent network, followed by addition of base to trigger cross-linking. Each step was confirmed to be complete after 24 h at 40 °C by both mechanical and spectroscopic measurements. The final interpenetrating network hydrogels consisted of a 23 wt % covalent network and 10 wt % coordination network.

The ability to prepare the HOPO-based coordination networks either alone or as an IPN then allowed a direct comparison of the physical and mechanical properties with the rheological properties of the coordination network being initially studied. Previously, the dissociation kinetics of the coordination bonds were shown to be a principle determinant of the viscoelastic behavior of coordination-based hydrogels.¹³ As a result, we hypothesized that by using different trivalent metal ions with different exchange kinetics with HOPO the lifetime over which these bonds are mechanically active could be controlled. This would allow hydrogels with tunable, strain-rate-dependent stiffening and recovery to be obtained. Three metal ions with similarly high affinity for 3,4-HOPO ligands but varying water exchange rates were chosen: Al^{3+} ($\log \beta = 34$, $k_{\text{exchange}} = 1 \text{ s}^{-1}$), Fe^{3+} ($\beta = 37$, $k_{\text{exchange}} = 200 \text{ s}^{-1}$), and In^{3+} ($\beta = 33$, $k_{\text{exchange}} = 10^6 \text{ s}^{-1}$).^{24–27}

Comparison of coordination hydrogels formed under the same conditions illustrates that linear viscoelastic oscillatory shear behavior is observed for hydrogels formed from Al^{3+} , Fe^{3+} , and In^{3+} -HOPO coordination cross-links at pH 8.2

(Figure 2). Significantly, all gels show predominantly elastic behavior at high ω and similar plateau moduli ($G'_{\text{plateau}} = 18.9\text{--}$

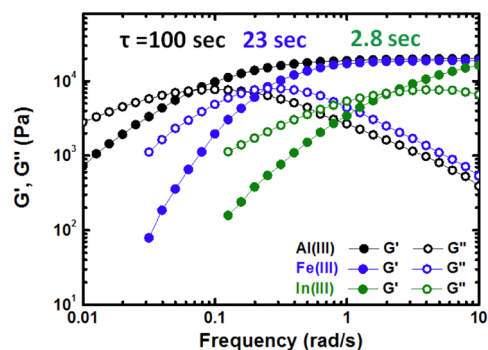


Figure 2. Dynamic shear moduli (G' , closed symbols; G'' , open symbols) as a function of frequency for $\text{Al}(\text{III})$ -, $\text{Fe}(\text{III})$ -, and $\text{In}(\text{III})$ -based HOPO hydrogels at pH 8.2.

21.3 kPa); however, the gels differ in relaxation time τ ($\tau = 1/G''_{\text{max}}$) by over two orders of magnitude, in a manner that follows measured water exchange kinetics.

Next, we looked to characterize the capacity for energy dissipation within the coordination network, as conveyed by the activation energy of viscoelasticity, by measuring the frequency-dependent rheological properties at a range of temperature $T = 15\text{--}45$ °C. We found that the viscoelastic moduli G' and G'' followed time-temperature superposition and collapsed onto a master curve by applying horizontal shift factors a_T (Figure 3a and b). Furthermore, this master curve ($T_{\text{ref}} = 45$ °C) is well fit by a single-relaxation Maxwell model, with $G'_{\text{plateau}} = 21.9 \text{ kPa}$ and $\tau = 2.95 \text{ s}$. This suggests that the viscoelasticity is primarily

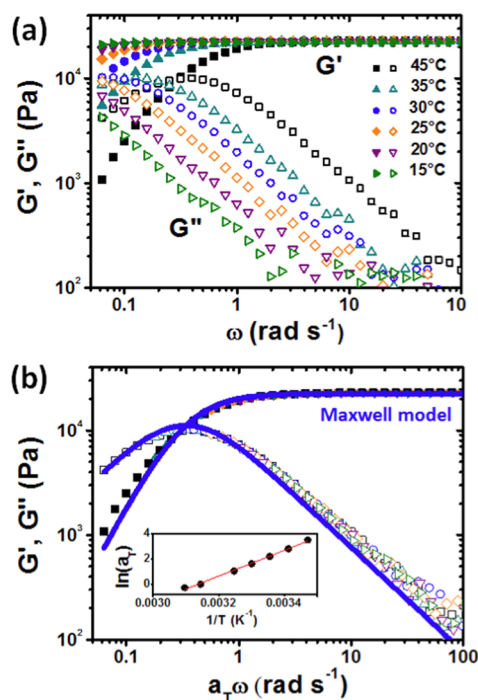


Figure 3. (a) Dynamic shear moduli of Al^{3+} -HOPO coordination hydrogel (pH 8.2) as a function of frequency from 15 to 45 °C. (b) Frequency sweeps shifted horizontally to fall onto a master curve which is well-fit by a single relaxation Maxwell model. Inset: Arrhenius plot of horizontal shift factor a_T with reference temperature of 45 °C.

determined by the cross-links, with minimal effect of chain entanglement in this dilute, highly swollen network. A plot of $\ln(a_T)$ versus inverse absolute temperature (inset in Figure 3b) follows a linear relationship over the range of temperatures tested. This shows that the hydrogel viscoelasticity exhibits Arrhenius behavior as described by the equation

$$\ln(a_T) = \frac{E_a}{R} \left(\frac{1}{T} - \frac{1}{T_{\text{ref}}} \right)$$

The slope of the linear fit allows us to determine an activation energy of viscoelasticity of 34 kT in this system, which is approximately 1/2 of the total energy of complex formation ($\Delta G_{\text{HOPO-Al(III)}} = 78$ kT). This value is comparable to other strong noncovalent interactions such as biotin–avidin (35 kT)²⁸ and gold–thiol bonds (35kT) and significantly higher than Upy-based quadruple H-bonding groups (18 kT in chloroform).^{29–31} In addition, the fraction of elastically effective cross-links in the pure HOPO-based hydrogels was determined to be 72% by comparison of the observed plateau modulus to the theoretical plateau modulus in this system, as described by

$$G = \rho RT$$

where ρ is equal to the maximum theoretical cross-link density.

This detailed rheological characterization of HOPO-based coordination networks highlights several promising features for use as energy dissipative materials. Namely:

- (1) individual cross-links have a high binding energy
- (2) use of different metal ions leads to tunable effective bond lifetimes
- (3) dynamic nature of the coordination bonds allows for network recovery and self-healing

In order to fully realize the potential of coordination bonds, we incorporated this coordination network with a covalent scaffold to form an interpenetrating network, as depicted in Figure 1. We envisioned the two components performing cooperatively, with the more highly cross-linked coordination network rupturing sacrificially and the loosely cross-linked covalent network providing an elastic restoring force after deformation.

The coordination-covalent IPNs were tested in both compression and tension. Figure 4a shows the results of compression tests on Fe^{3+} –HOPO IPNs carried out to 80% strain at a constant compression and unloading speed corresponding to an initial strain rate of 4 mm/mm min⁻¹. The curves for the IPN without Fe^{3+} added and with Fe^{3+} at pH 3 are similar and show predominantly elastic behavior, with ~15% energy dissipation on unloading. Upon raising the pH to 8.2, the work of loading increases by a factor of 2.5, as both the modulus and stress at 80% strain show a substantial increase. Furthermore, the sample exhibits a larger hysteresis upon unloading, corresponding to ~50% energy dissipation. These observations illustrate the mechanical contribution to the hydrogel due to cross-linking of the coordination network. Similar effects are notable in mechanical testing in tension, as depicted in Figure 4b.

To demonstrate the strain rate and metal-dependent reinforcement provided by the coordination network, IPN samples were made with Al^{3+} , Fe^{3+} , and In^{3+} and measured at varying compression rates. The shear compressive modulus was found to be constant at low strains, well described by the statistical thermodynamic treatment of rubber elasticity

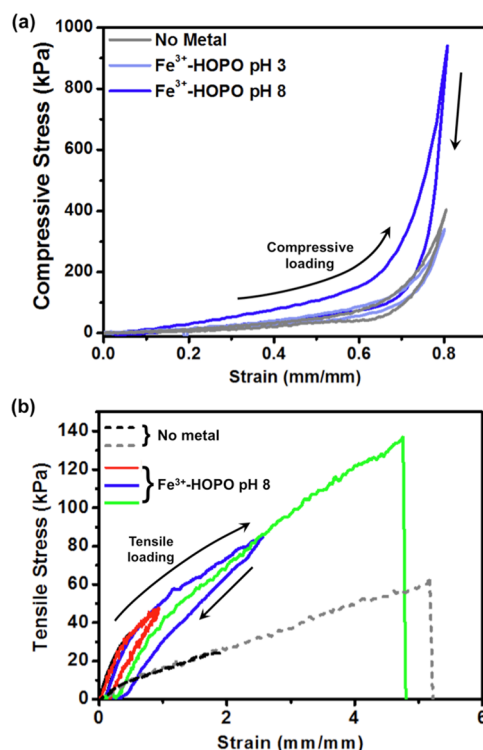


Figure 4. (a) Compressive stress/strain curves for the interpenetrating network without Fe^{3+} added (gray), with Fe^{3+} at low pH (light blue), and at high pH (dark blue). (b) Tensile stress/strain curves upon consecutive loadings to increasing extensions. Dotted lines are the interpenetrating network without metal, and the solid lines are with Fe^{3+} added (pH 8.2).

$$G = \frac{\tau}{\lambda - \lambda^{-2}}$$

where τ is the compressive stress and λ is the extension ratio. Moduli were extracted from the linear fit of the τ versus $\lambda - \lambda^{-2}$ plot for strains between 5 and 25% and summarized in Figure 5. Without metal, the initial compressive shear modulus was 11.8 ± 0.4 kPa and was unchanged within error for strain rates from 0.01 to 4 mm/mm min⁻¹. The addition of metals and base triggered formation of the coordination network. Upon compression, we observed clear strain rate dependence. IPNs

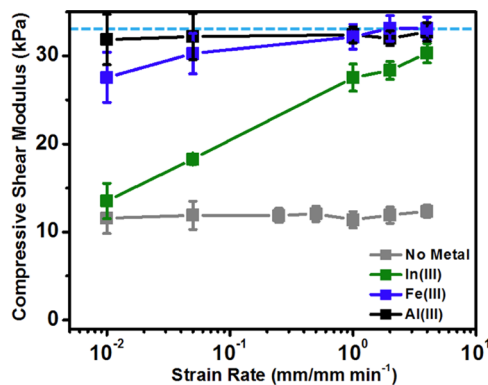


Figure 5. Initial compressive shear modulus as a function of strain rate for interpenetrating network hydrogels with no metal and In(III), Fe(III), and Al(III) at pH 8.2. The blue dotted line represents the additive sum of the covalent acrylamide network and the shear plateau modulus of the coordination network.

with In^{3+} –HOPO coordination networks showed a minimally higher modulus than without metal at low strain rates ($G = 16.1 \pm 2.0$ kPa) but tended toward the additive moduli of the coordination and covalent network as the strain rate increases to 4 mm/mm min^{-1} ($G = 30.4 \pm 1.4$ kPa). Compression of IPNs incorporating the more kinetically inert metals, Fe^{3+} and Al^{3+} , exhibited less strain rate-dependent moduli over the range of accessible rates, though it should be noted that Fe^{3+} –HOPO IPN hydrogels softened at low strain rates.

Having demonstrated that incorporation of the coordination network leads to strain-rate- and metal-dependent changes in mechanical response, we leveraged this control to create IPNs with tunable recovery dynamics. Figure 6 shows the extracted

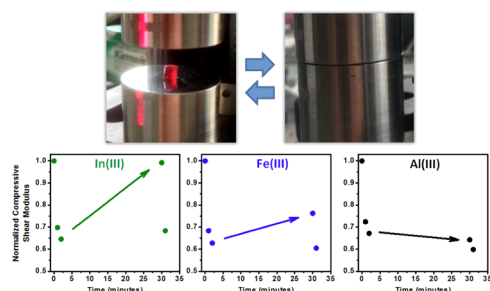


Figure 6. Measurement of initial compressive modulus upon repeated cycling to 80% compression, followed by a 30 min recovery period.

initial moduli from three consecutive compression cycles to 80% strain, followed by a 30 min recovery period. All hydrogels show lower initial moduli, signifying rupture of cross-links, upon repeated cycling. IPN hydrogels with labile In^{3+} cross-linking heal rapidly, recovering to 99% of their initial modulus after 30 min rest (Figure S2). Fe^{3+} IPNs show partial recovery after 30 min, while Al^{3+} hydrogels remain damaged. Cyclic compression to 80% strain shows no damage in the covalent network alone.

In summary, we have taken advantage of high-affinity coordination cross-links to introduce rate-dependent, recoverable reinforcement in an interpenetrating network hydrogel. Pure coordination networks exhibit high activation energy of flow and allow for direct correlation between coordination chemistry and bulk mechanical properties. The effective bond lifetimes of these networks are dependent upon complex dissociation and can be varied over 2 orders of magnitude by using several different hard, trivalent metal ions with varying kinetic lability. To address the brittle, dynamic nature of this system, coordination networks were incorporated into a loosely cross-linked covalent scaffold. The mechanical properties of these IPN hydrogels blend the properties of the covalent and the coordination networks. The coordination networks provide stiffness and energy dissipation at strain rates above their characteristic relaxation time and minimal reinforcement at slow rates. Labile In^{3+} -coordinate hydrogels are damaged by repeated compressive cycles but recover over the course of 30 min. IPN hydrogels with Fe^{3+} and Al^{3+} show slower recovery dynamics. This work highlights that the incorporation of a small amount of high-affinity coordination complexes can impart significant changes in mechanical properties in IPN hydrogels.

■ ASSOCIATED CONTENT

Supporting Information

The Supporting Information is available free of charge on the ACS Publications website at DOI: 10.1021/acsmacrolett.5b00664.

Experimental details, ^1H NMR spectrum of the PEG–HOPO cross-linker, and raw tensile and compressive test data (PDF)

■ AUTHOR INFORMATION

Corresponding Author

*E-mail: herbert.waite@lifesci.ucsb.edu.

Notes

The authors declare no competing financial interest.

■ ACKNOWLEDGMENTS

This work was supported by the Materials Research Science and Engineering Centers Program of the National Science Foundation under Award no. DMR 1121053 and by a grant from the National Institutes of Health R01 DE018468 (JHW).

■ REFERENCES

- (1) Degtyar, E.; Harrington, M. J.; Politi, Y.; Fratzl, P. *Angew. Chem., Int. Ed.* **2014**, *53* (45), 12026–12044.
- (2) Holten-Andersen, N.; Zhao, H.; Waite, J. H. *Biochemistry* **2009**, *48* (12), 2752–2759.
- (3) Holten-Andersen, N.; Fantner, G. E.; Hohlbauch, S.; Waite, J. H.; Zok, F. W. *Nat. Mater.* **2007**, *6* (9), 669–672.
- (4) Gosline, J.; Lillie, M.; Carrington, E.; Guerette, P.; Ortlepp, C.; Savage, K. *Philos. Trans. R. Soc., B* **2002**, *357* (1418), 121–132.
- (5) Vaccaro, E.; Waite, J. *Biomacromolecules* **2001**, *2* (3), 906–911.
- (6) Harrington, M. J.; Waite, J. H. *J. Exp. Biol.* **2007**, *210*, 4307–4318.
- (7) Ashton, N. N.; Stewart, R. J. *Soft Matter* **2015**, *11* (9), 1667.
- (8) Krogsgaard, M.; Behrens, M. a.; Pedersen, J. S.; Birkedal, H. *Biomacromolecules* **2013**, *14* (2), 297–301.
- (9) Krogsgaard, M.; Hansen, M. R.; Birkedal, H. *J. Mater. Chem. B* **2014**, *2* (47), 8292–8297.
- (10) Barrett, D. G.; Fullenkamp, D. E.; He, L.; Holten-Andersen, N.; Lee, K. Y. C.; Messersmith, P. B. *Adv. Funct. Mater.* **2013**, *23*, 1111–1119.
- (11) Fullenkamp, D. E.; He, L.; Barrett, D. G.; Burghardt, W. R.; Messersmith, P. B. *Macromolecules* **2013**, *46* (3), 1167–1174.
- (12) Holten-Andersen, N.; Jaishankar, A.; Harrington, M. J.; Fullenkamp, D. E.; DiMarco, G.; He, L.; McKinley, G. H.; Messersmith, P. B.; Lee, K. Y. C. *J. Mater. Chem. B* **2014**, *2* (17), 2467.
- (13) Yount, W. C.; Loveless, D. M.; Craig, S. L. *J. Am. Chem. Soc.* **2005**, *127* (41), 14488–14496.
- (14) Yount, W.; Juwarker, H.; Craig, S. J. *J. Am. Chem. Soc.* **2003**, *125*, 15302–15303.
- (15) Martell, A.; Smith, R. *Critical Stability Constants*; Plenum Press: New York, 1977.
- (16) Wei, Z.; He, J.; Liang, T.; Oh, H.; Athas, J.; Tong, Z.; Wang, C.; Nie, Z. *Polym. Chem.* **2013**, *4* (17), 4601.
- (17) Henderson, K. J.; Zhou, T. C.; Otim, K. J.; Shull, K. R. *Macromolecules* **2010**, *43* (14), 6193–6201.
- (18) Pan, Y.; Gao, Y.; Shi, J.; Wang, L.; Xu, B. *J. Mater. Chem.* **2011**, *21* (19), 6804.
- (19) Sun, J.-Y.; Zhao, X.; Illeperuma, W. R. K.; Chaudhuri, O.; Oh, K. H.; Mooney, D. J.; Vlassak, J. J.; Suo, Z. *Nature* **2012**, *489* (7414), 133–136.
- (20) Grindy, S. C.; Learsch, R.; Mozhdzhi, D.; Cheng, J.; Barrett, D. G.; Guan, Z.; Messersmith, P. B.; Holten-Andersen, N. *Nat. Mater.* **2015**, 1–8.

- (21) Menyo, M.; Hawker, C.; Waite, J. *Soft Matter* **2013**, *9*, 10314–10323.
- (22) Webber, R. E.; Creton, C.; Brown, H. R.; Gong, J. P. *Macromolecules* **2007**, *40*, 2919–2927.
- (23) Truong, V. X.; Ablett, M. P.; Richardson, S. M.; Hoyland, J. A.; Dove, A. P. *J. Am. Chem. Soc.* **2015**, *137* (4), 1618–1622.
- (24) Helm, L.; Merbach, A. E. *Coord. Chem. Rev.* **1999**, *187* (1), 151–181.
- (25) Clevette, D.; Lyster, D.; Nelson, W.; et al. *Inorg. Chem.* **1990**, *29* (4), 667–672.
- (26) Chaves, S.; Gil, M.; Marques, S.; Gano, L.; Santos, M. A. *J. Inorg. Biochem.* **2003**, *97* (1), 161–172.
- (27) Dobbin, P. S.; Hider, R. C.; Hall, a D.; Taylor, P. D.; Sarpong, P.; Porter, J. B.; Xiao, G.; van der Helm, D. *J. Med. Chem.* **1993**, *36* (17), 2448–2458.
- (28) Green, N. *Biochem. J.* **1966**, *101*, 774–780.
- (29) Folmer, B. J. B.; Sijbesma, R.; Kooijman, H.; Spek, A. L.; Meijer, E. W. *J. Am. Chem. Soc.* **2000**, *121*, 9001–9007.
- (30) Guo, M.; Pitet, L. M.; Wyss, H. M.; Vos, M.; Dankers, P. Y. W.; Meijer, E. W. *J. Am. Chem. Soc.* **2014**, *136* (19), 6969–6977.
- (31) Dankers, P. Y. W.; Meijer, E. W.; et al. *Adv. Mater.* **2012**, *24* (20), 2703–2709.